Kovove Mater. 50 2012 393–397
DOI: 10.4149/km_2012_6_393

High-temperature mechanical properties of AZ61 and AZ61-0.7Si magnesium alloys

A. R. Geranmayeh, R. Mahmudi*, A. Movahedi-Rad, M. H. Malekoshoaraei

School of Metallurgical and Materials Engineering, College of Engineering, University of Tehran, Tehran, Iran

Received 2 March 2012, received in revised form 15 September 2012, accepted 17 September 2012

Abstract

The effects of 0.7 wt.% Si addition on the microstructural evolution, hardness, creep resistance, and shear strength of AZ61 alloy were investigated in the temperature range 298–523 K. Creep behavior was assessed by impression creep test, and ultimate shear strength (USS) was measured by the shear punch test (SPT). The as-cast structure of AZ61 consists of α-Mg matrix and the β-$Mg_{17}Al_{12}$ intermetallic phase. Due to the low thermal stability of this phase, the hardness and strength of AZ61 significantly decreased as the temperature increased. The results showed that hot hardness, creep resistance and high-temperature shear strength of the base alloy were significantly enhanced with the addition of Si. This was attributed to the reduction in the volume fraction of β-$Mg_{17}Al_{12}$ and formation of the more thermally stable Mg_2Si intermetallic particles. These particles have a Chinese script morphology which reduce ductility but act as the main strengthening agent in the investigated system, by strengthening the matrix of the base alloy and hindering grain growth during deformation.

Key words: AZ61 Mg alloy, shear strength, creep, hardness

1. Introduction

Magnesium alloys, as the lightest structural metallic materials, are of special interest in automobile, aerospace, and electronic industries [1]. The most common types of these materials are those based on the Mg-Al system [2, 3]. These alloys possess a combination of attractive properties such as low density, high specific strength, specific stiffness, good castability, and reasonable cost [4]. Despite these advantages, Mg-Al alloys have relatively poor mechanical properties at elevated temperatures, mainly due to the thermal instability of microstructure containing $Mg_{17}Al_{12}$ phase [2, 5, 6]. Accordingly, attention has been directed towards developing new alloys with enhanced high-temperature mechanical properties. This has often been achieved by introducing alloying elements such as Ca, RE, Zn, Sb, and Si, which are capable of forming thermally stable intermetallics in the magnesium matrix.

Si is one of the most promising alloying elements, which can form the Mg_2Si intermetallic compound with a high melting point of 1085 ℃ [7]. This stable phase, which exists only at stoichiometric composition, possesses low density, high elastic modulus, and low thermal expansion coefficients [8]. However, Mg_2Si compound is prone to form as coarse Chinese script particles under low solidification rates. This morphology, which results in easy nucleation of cracks along the interface between Mg_2Si intermetallic particles and α-Mg matrix, is believed to be detrimental to mechanical properties [9, 10]. Therefore, attempts have been made to change the Chinese script morphology of Mg_2Si particles into globular or cuboid in the Mg alloys. This can be achieved by either special heat treatments or compositional changes made into the Mg alloy melt, both of which could impose extra costs on the manufacturing of the final parts. Although it is now evident that the modified Mg_2Si phase can be beneficial to both creep resistance [11] and high-temperature mechanical properties [12, 13], the investigation of mechanical properties of Mg-Al-Si cast alloys containing coarse Mg_2Si particles is still of some importance due to cost efficiency concerns. The aim of this study is thus to investigate the effects of 0.7 wt.% Si addition on the microstructure, and elev-

*Corresponding author: tel.: +98 21 8208 4137; fax: +98 21 8800 6076; e-mail address: mahmudi@ut.ac.ir

ated temperature mechanical properties of the AZ61 alloy in the as-cast condition.

2. Experimental procedure

The materials used were AZ61 alloy with an actual chemical composition of Mg-6.1wt.%Al-0.82wt.%Zn--0.30wt.%Mn, and the same material with 0.7 wt.% Si addition. High purity Mg, Zn, Mn, and an Al--15wt.%Si master alloy were used to prepare the alloys. Melting was carried out in a graphite crucible placed in an electrical resistance furnace under the Foseco Magrex 36 covering flux, to protect molten magnesium from oxidation. The melt was held at 750 ℃ for 20 min and mechanically stirred for 2 min to ensure a homogeneous composition. Pouring was accomplished into a steel die preheated up to 300 ℃. The cast slabs had dimensions of 13 mm × 30 mm × 120 mm, from which 3-mm thick slices were cut by an electrodischarge wire--cut machine for shear punch test (SPT), impression creep, and structural characterization. Scanning electron microscopy (SEM) was used to reveal the microstructural features of the alloys. X-ray diffraction analysis was carried out on selected samples to identify the constitutive phases of each alloy.

A universal tensile testing machine equipped with a three-zone split furnace was used to perform impression creep, shear punch, and hot hardness tests in the air atmosphere. The details of testing arrangement of these tests are explained elsewhere [14–16] and will only be briefly described here. In impression creep tests, a flat-ended cylindrical punch 2 mm in diameter was mounted in a holder positioned in the center of the vertical loading bar. The specimen was located on an anvil below the loading bar; the assembly of the specimen and the indenter was accommodated by the split furnace. Measurements were made on each sample at 200 ℃ and under punch stress of 350 MPa for dwell times up to 4000 s. After application of the load, the impression depth was measured automatically as a function of time by the machine; the data were acquired by a computer.

The same configuration was used for the hot hardness tests, in which a Vickers indenter was mounted in the holder instead of the flat-ended punch. A load of 10 N at an approaching rate of 0.5 mm min^{-1} was applied for a dwell time of 30 s. At least three indentations were made on each sample and the average lengths of the diagonals were used to estimate the hardness values in the temperature range 25–250 ℃. The thin slices of the as-cast materials were ground to a thickness of 0.6 mm, from which disks of 10 mm in diameter were punched for the shear punch test. A shear punch fixture with a 3.175 mm diameter flat cylindrical punch and 3.225 mm diameter receiving hole was used for this experiment. Shear punch tests were performed in the temperature range 25–250 ℃ using a constant cross-head speed of 0.25 mm min^{-1}. The applied load P was measured automatically as a function of punch displacement; the data were acquired by a computer so as to determine the shear stress of the tested materials using the relationship [17]:

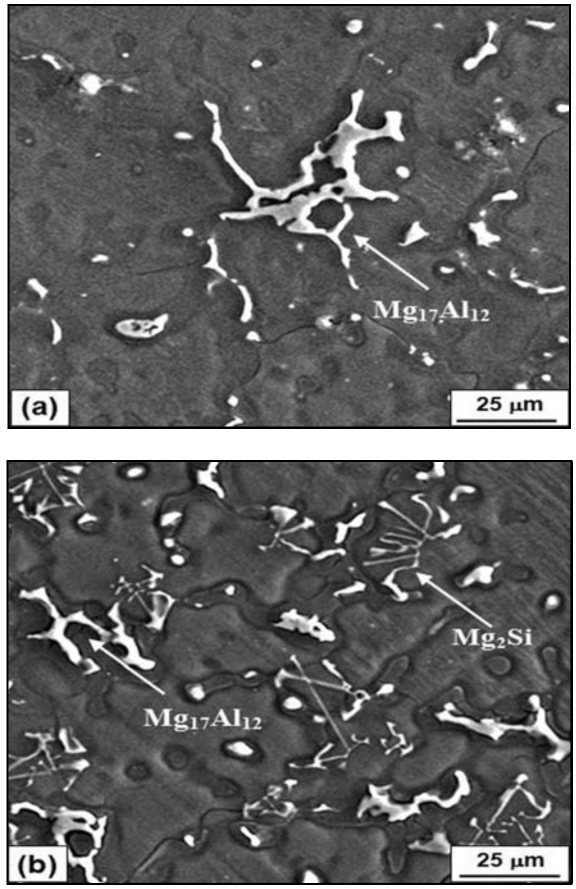

Fig. 1. SEM micrographs of: (a) AZ61, and (b) AZ61-0.7Si alloys in the as-cast condition.

$$\tau = \frac{P}{\pi d t}, \tag{1}$$

where P is the punch load, t is the specimen thickness and d is the average of the punch and die hole diameters.

3. Results and discussion

The as-cast microstructures of the tested materials revealed by SEM are shown in Fig. 1. As can be seen in Fig. 1a, the base AZ61 alloy exhibits a dendritic microstructure with some bulky β-$Mg_{17}Al_{12}$ second phase particles formed in the interdendritic regions. Addition of 0.7 % Si to the base alloy results in a change

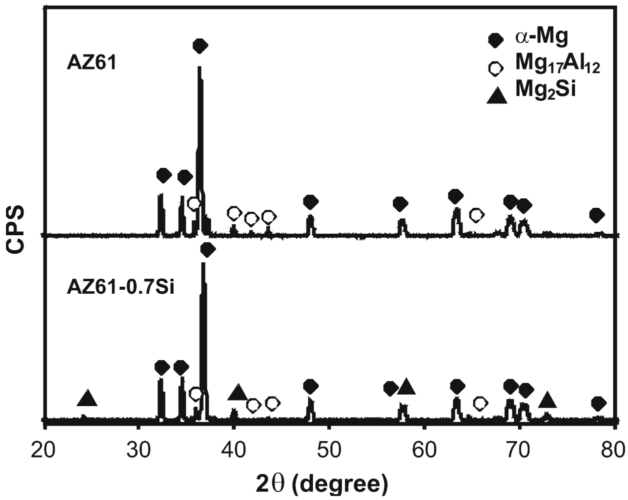

Fig. 2. XRD patterns of the AZ61 and AZ61-0.7Si alloys.

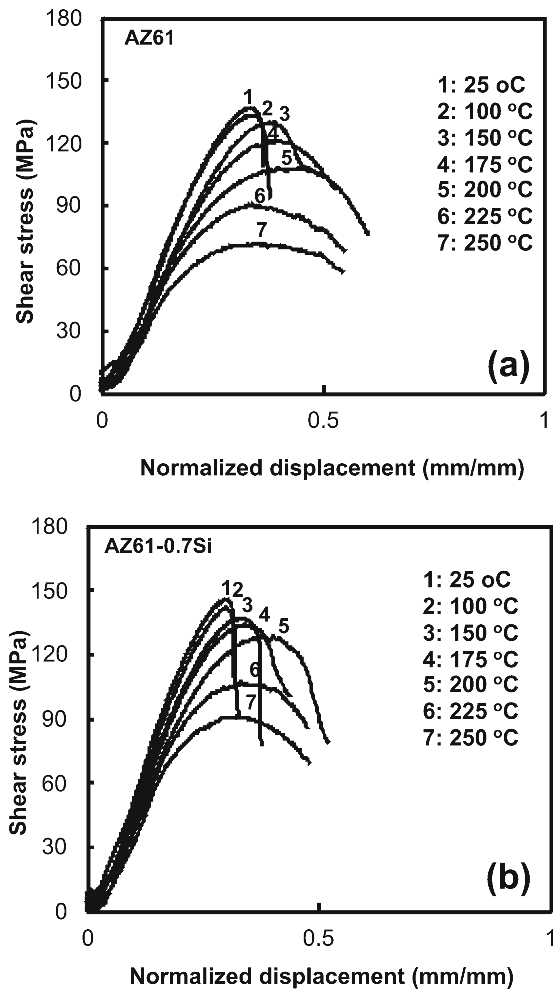

Fig. 3. SPT curves of: (a) AZ61, and (b) AZ61-0.7Si alloys obtained at different test temperatures.

in the size and distribution of these particles and the formation of Mg_2Si particles with the Chinese script morphology, as shown in Fig. 1b. Qualitative analysis of these particles, determined by the EDS analysis, indicated that these particles show the composition of $Mg_{67.5}Si_{32.5}$, which corresponds to the Mg_2Si compound. The X-ray diffraction analysis of the tested alloys, depicted in Fig. 2, reveals the phases present in each material. It is observed that α-Mg and the β-$Mg_{17}Al_{12}$ intermetallic compounds are the only constitutes of the base alloy, while some low intensity new peaks, corresponding to the Mg_2Si phase, can be observed in the XRD pattern of the Si-containing alloy.

The SPT technique, which has been recently used for cast magnesium alloys [18, 19], is an efficient method that is capable of collecting strength data which are well correlated with the conventional tensile test data [20–22]. Figures 3a,b exhibit the variation of shear stress with normalized displacement obtained at different temperatures for AZ61 and AZ61-0.7Si alloys, respectively. It can be observed that, similar to conventional tensile stress-strain curves, after a linear elastic behavior the curves deviate from linearity before they reach a maximum point. The stress corresponding to the maximum point is referred to as the ultimate shear strength (USS). In both materials studied in this work, increasing the test temperature from 25 to 250 ℃ results in lower USS values, the effect of which is more pronounced in the AZ61 alloy.

To have an overall view on the variation of strength with temperature, the USS data of both materials obtained at different test temperatures are shown in Fig. 4a. Although the general trend of USS drop with increasing test temperature is to some extent similar for both alloys, the Si-containing alloy possesses higher strength levels at all investigated temperatures. Similar trends in the variation of hardness with temperature are exhibited in Fig. 4b. It can be seen that there is a gradual decrease in both strength and hardness values up to about 150 ℃, after which a steeper drop in these properties is evident. The observed softening behavior can be attributed to the operative strengthening mechanisms in the Mg-Al alloys. These mechanisms are namely the solid solution strengthening effects of Al in Mg, and the second-phase strengthening stemmed from the formation of Mg-Al phase. A portion of the added aluminum dissolves into the Mg matrix and improves the mechanical properties of magnesium through solid solution hardening [3]. Solid solution strengthening effects, however, disappear at high temperatures due to the high diffusion rate of Al in Mg. For aluminum contents higher than 2 wt.%, a new β-$Mg_{17}Al_{12}$ phase could form as particles and precipitates, improving room-temperature mechanical properties of the alloys by hindering dislocation movements. However, $Mg_{17}Al_{12}$ particles have low thermal stability because of their low melting point (437 ℃) and tend to dissolve at above 130 ℃. These arguments are in agreement with our results on the strength and

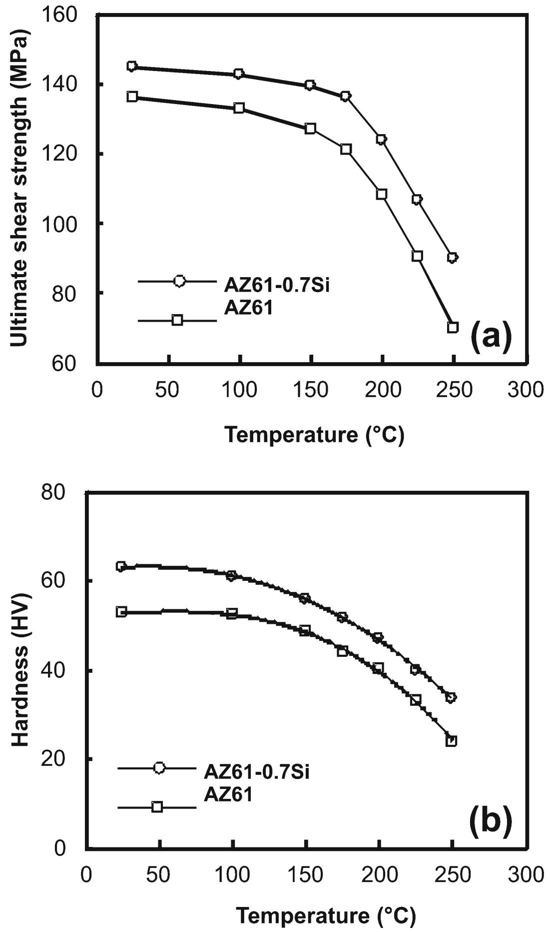

Fig. 4. Variation of: (a) ultimate shear strength, and (b) hardness with test temperature for the AZ61 and AZ61-0.7Si alloys.

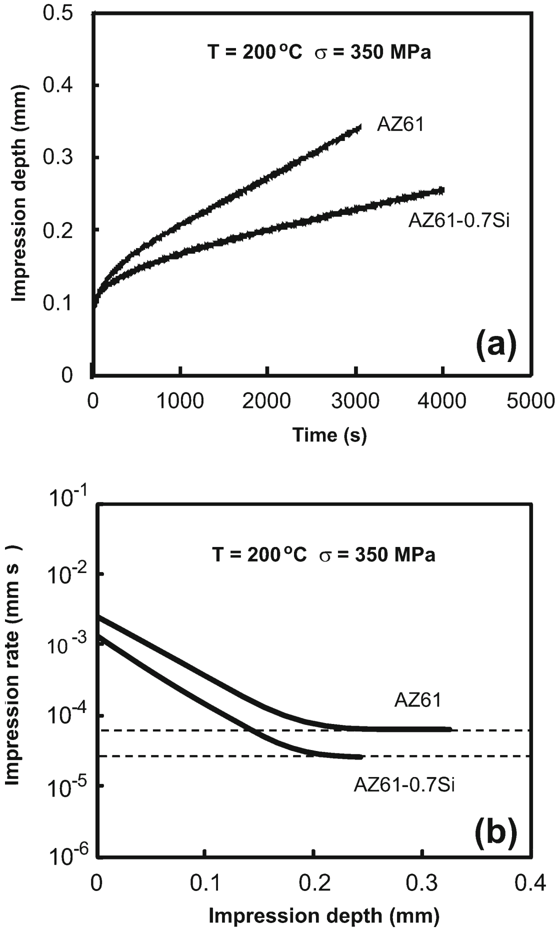

Fig. 5. Comparison of: (a) creep behavior, and (b) minimum creep rates of the investigated alloys at $T = 200\,^{\circ}\mathrm{C}$ and $\sigma = 350$ MPa.

hardness of the tested alloys, which show a weaker dependence on the test temperature up to about 150 °C, and a pronounced drop at higher temperatures. The higher strength and hardness of the AZ61-0.7Si alloy is ascribed to the formation of the high melting point Mg_2Si second-phase particles. These thermally stable particles are mainly responsible for the enhanced strength and hardness of the Si-containing alloy at all temperatures.

Results of impression creep tests of the investigated alloys, obtained at 200 °C under the punch stress of 350 MPa, are shown in Fig. 5. As shown in Fig. 5a, there is a rather wide gap between the curves of the two alloys. It can further be seen that after a rather short primary creep stage, both alloys show a secondary-state region where depth increases linearly with time. Since the impression test is essentially compressive in nature, fracture of the specimen does not occur, and hence, it is obviously not possible to record a third stage of the curve, as would be possible in conventional tensile creep testing. However, it is possible to find the minimum creep rates by differentiating the creep data with respect to time. The time derivatives of the creep curves were thus calculated by a five-point cubic spline numerical differentiation computer program.

For comparison of the creep behavior of the materials, their impression creep rates are plotted under the punch stress of 350 MPa at 200 °C in Fig. 5b. The lower level and slope in the steady-state region of the curve of the Si-containing alloy in Fig. 5a is translated to a lower impression rate in Fig. 5b. It can be inferred that the addition of Si significantly improves the creep resistance of the base alloy by lowering its impression creep rate. This is evident from the lower impression rate of the AZ61-0.7Si alloy, as compared to the AZ61 base alloy. Similar to the shear strength and hot hardness behavior, shown in Fig. 4, the improved creep resistance of AZ61-0.7Si is attributed to the presence of the high melting point Mg_2Si particles with sufficient thermal stability, acting as high temperature strengthening particles. This is in contrast to the lower creep resistance of the AZ61 alloy, in which the low thermal stability of $Mg_{17}Al_{12}$ particles can accelerate grain boundary diffusion and cause remarkable instability of the microstructure in regions adjacent to grain boundaries [23].

4. Conclusions

The microstructural evolution, creep resistance, hot hardness and high temperature shear strength of the AZ61 and AZ61-0.7Si alloys were investigated in the as-cast condition. Microstructural analysis showed that the microstructure of AZ61 contained $Mg_{17}Al_{12}$ intermetallic phase in the Mg matrix, while addition of 0.7 wt.% Si elements resulted in the formation of Chinese script Mg_2Si particles. The low thermal stability of the eutectic β-$Mg_{17}Al_{12}$ phase resulted in the softening of both alloys during exposure to high temperature. Addition of 0.7 % Si to the base alloy increased the hardness, shear strength, and creep resistance of the alloy, mainly due to the formation of Mg_2Si particles with the Chinese script morphology. These particles are thermally stable and strengthen both grains and grain boundaries and oppose both recovery and recrystallization processes during deformation processes at elevated temperatures, decreasing the minimum creep rate and increasing the hardness and strength of the material.

Acknowledgement

The authors thank the Iran National Science Foundation (INSF) for providing financial support of this work under Grant No. 89084/87.

References

[1] Mordike, B. L., Ebert, T.: Mater. Sci. Eng., *A302*, 2001, p. 37. doi:10.1016/S0921-5093(00)01351-4
[2] Trojanová, Z., Lukáč, P., Kainer, K. U.: Adv. Eng. Mater., *9*, 2007, p. 370. doi:10.1002/adem.200700018
[3] Kondori, B., Mahmudi, R.: Metall. Mater. Trans., *40A*, 2009, p. 2007. doi:10.1007/s11661-009-9867-4
[4] Luo, A. A.: Int. Mater. Rev., *49*, 2004, p. 13. doi:10.1179/095066004225010497
[5] Kondori, B., Mahmudi, R.: Mater. Sci. Eng., *A527*, 2010, p. 2014. doi:10.1016/j.msea.2009.11.043
[6] Mahmudi, R., Kabirian, F., Nematollahi, Z.: Mater. Des., *32*, 2011, p. 2583. doi:10.1016/j.matdes.2011.01.040
[7] ASM Handbook, Vol. 3, 1992.
[8] Lu, Y. Z., Wang, Q. D., Zeng, X. Q., Zhu, Y. P., Ding, W. J.: Mater. Sci. Technol., *17*, 2001, p. 207. doi:10.1179/026708301101509872
[9] Kim, J. J., Kim, D. H., Shin, K. S., Kim, N. J.: Scripta Mater., *41*, 1999, p. 333. doi:10.1016/S1359-6462(99)00172-4
[10] Alizadeh, R., Mahmudi, R.: J. Alloys Compd., *509*, 2011, p. 9195. doi:10.1016/j.jallcom.2011.06.109
[11] Srinivasan, A., Pillai, U. T. S., Pai, B. C.: Metall. Mater. Trans., *36A*, 2005, p. 2235. doi:10.1007/s11661-005-0342-6
[12] Arunachaleswaran, A., Pereira, I. M., Dieringa, H., Huang, Y., Hort, N., Dhindaw, B. K., Kainer, K. U.: Mater. Sci. Eng., *A460–461*, 2007, p. 268. doi:10.1016/j.msea.2007.01.043
[13] Ding, S. S., Din, G. C., Hua, C. Z.: J. Alloy Compd., *470*, 2009, p. L17. doi:10.1016/j.jallcom.2008.03.005
[14] Mahmudi, R., Geranmayeh, A. R., Rezaee-Bazzaz, A.: Mater. Sci. Eng., *A448*, 2007, p. 287. doi:10.1016/j.msea.2006.10.092
[15] Alizadeh, R., Mahmudi, R.: Mater. Sci. Eng., *A527*, 2010, p. 3975. doi:10.1016/j.msea.2010.03.007
[16] Keyvani, M., Mahmudi, R., Nayyeri, G.: Mater. Sci. Eng., *A527*, 2010, p. 7714. doi:10.1016/j.msea.2010.08.045
[17] Hankin, G. L., Toloczko, M. B., Johnson, K. I., Khaleel, M. A., Hamilton, M. L., Garner, F. A., Davies, R. W., Faulkner, R. G.: 19th International Symposium, ASTM STP 1366, 1999, p. 1018.
[18] Nayyeri, G., Mahmudi, R., Salehi, F.: Mater. Sci. Eng., *A527*, 2010, p. 5353. doi:10.1016/j.msea.2010.05.040
[19] Golmakaniyoon, S., Mahmudi, R.: Mater. Sci. Eng., *A528*, 2011, p. 5228. doi:10.1016/j.msea.2011.03.083
[20] Guduru, R. K., Nagasekhar, A. V., Scattergood, R. O., Koch, C. C., Murty, K. L.: Metall. Mater. Trans., *37A*, 2006, p. 1477. doi:10.1007/s11661-006-0092-0
[21] Masoudpanah, S. M., Mahmudi, R.: Mater. Des., *3*, 2010, p. 3512. doi:10.1016/j.matdes.2010.02.018
[22] Masoudpanah, S. M., Mahmudi, R., Langdon, T. G.: Kovove Mater., *49*, 2011, p. 43. doi:10.4149/km_2011_1_43
[23] Kabirian, F., Mahmudi, R.: Adv. Eng. Mater., *11*, 2009, p. 189. doi:10.1002/adem.200800223